Supplemental Information

1. Gaussian Calculations

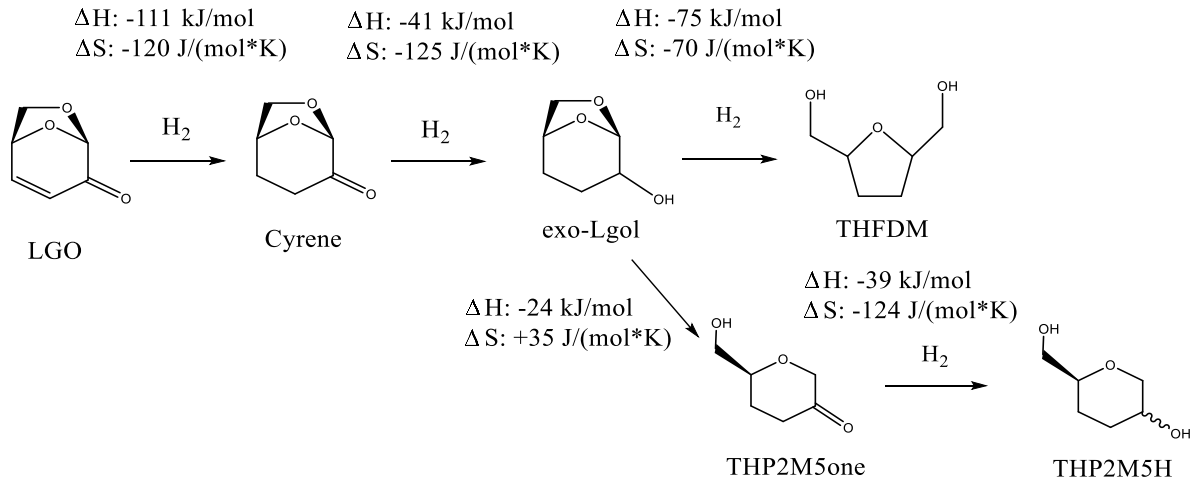

Scheme S1: LGO hydrogenation reaction network with ΔH and ΔS values for each reaction step (25°C) included, calculated from Gaussian.

Density functional theory calculations were performed in Gaussian V9[1] using the B3LYP/6-31G+(d,p) level of theory. A geometry optimization calculation was used to find the lowest energy configuration of each stable molecule and the thermochemistry associated with that configuration. A polarizable continuum model (PCM) was used to model a pseudo-solvent cage in order to approximate the effect of solvation by THF. Calculations were carried out at 25°C.

LGO hydrogenation to Cyrene is enthalpically favored by -111 kJ/mol. This value is in agreement with the enthalpy of hydrogenation of cyclohexene to cyclohexane in the literature (-118 kJ/mol).[2] The 2-enone functionality (present in LGO) adds an additional resonance stabilization of approximately 13 kJ/mol.[3] The entropies of reaction are also in moderate agreement with literature – we calculated an entropy change of -120 J/(mol*K) for LGO hydrogenation, while cyclohexene hydrogenation is associated with an entropy change of -143 J/(mol*K). Cyrene hydrogenation to Lgol is enthalpically favored by -41 kJ/mol, which is moderately smaller than the enthalpy of hydrogenation of cyclohexanone to cyclohexanol reported in the literature (-62 kJ/mol).[2] The entropies are comparable: our value is -125 J/(mol*K) while the literature value for cyclohexanone hydrogenation is -112 J/(mol*K).

Lgol hydrogenolysis to THFDM is enthalpically favored by -75 kJ/mol, whereas Lgol hydrogenolysis to THP2M5H is enthalpically favored by -64 kJ/mol. This difference of 11 kJ/mol is near the error of the Gaussian calculations, so conclusions cannot be drawn about whether THP2M5H or THFDM is the thermodynamically favored product. Lgol isomerization to THP2M5one is enthalpically favored by -24 kJ/mol. All sets of stereoisomers (exo-Lgol vs endo-Lgol; cis-THFDM vs trans-THFDM; cis-THP2M5H vs trans-THP2M5H), are very similar in energy, with enthalpies differing by < 3 kJ/mol. This is within the error of the Gaussian calculations.

2. ^{13}C NMR Spectra

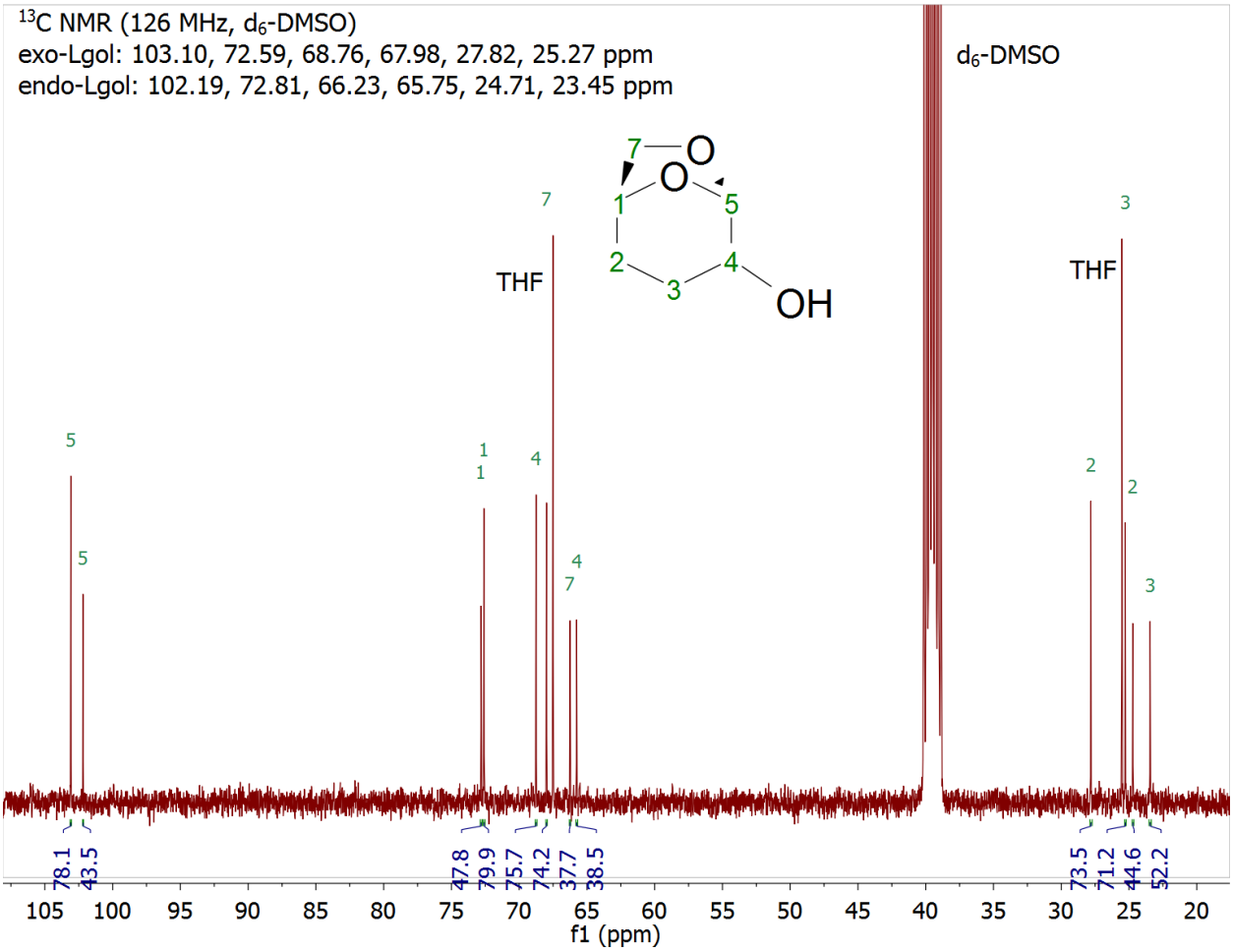

Figure S1: Quantitative ^{13}C NMR spectrum of Cyrene hydrogenation containing exo-Lgol and endo-Lgol (d$_6$-DMSO and residual THF solvent are also present). Multiplicities were confirmed using polarization transfer (DEPT) experiments. 480 Scans were used with a relaxation delay of 20 sec.

Measured chemical shifts agree with the literature.[4]

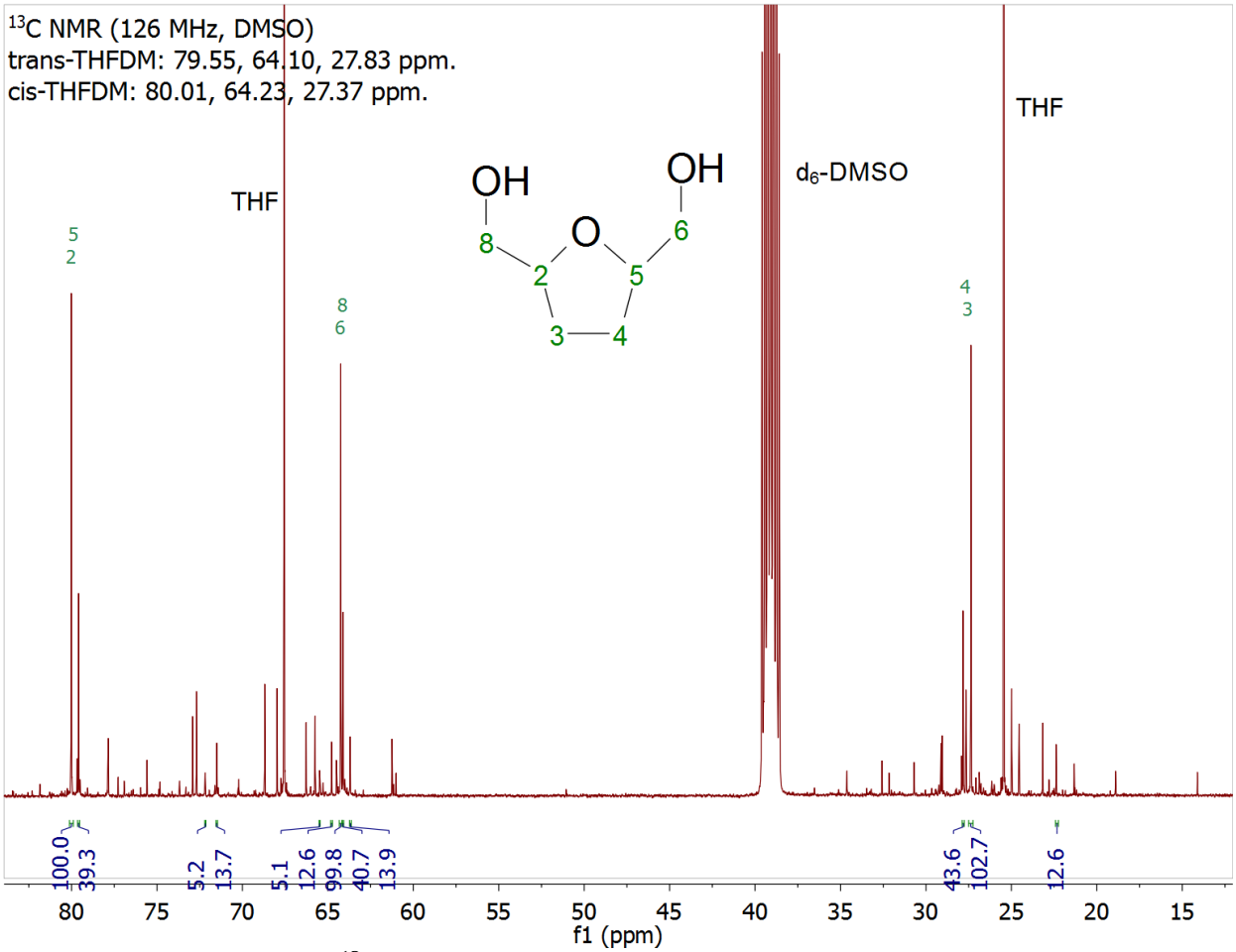

Figure S2: Quantitative ^{13}C NMR spectrum of THFDM-rich product, produced via Lgol hydrogenolysis in Figure 3. (d_6-DMSO, residual THF solvent, Lgol, other side-products are also present). Multiplicities were confirmed using polarization transfer (DEPT) experiments.

Measured chemical shifts agree with the literature.[5]

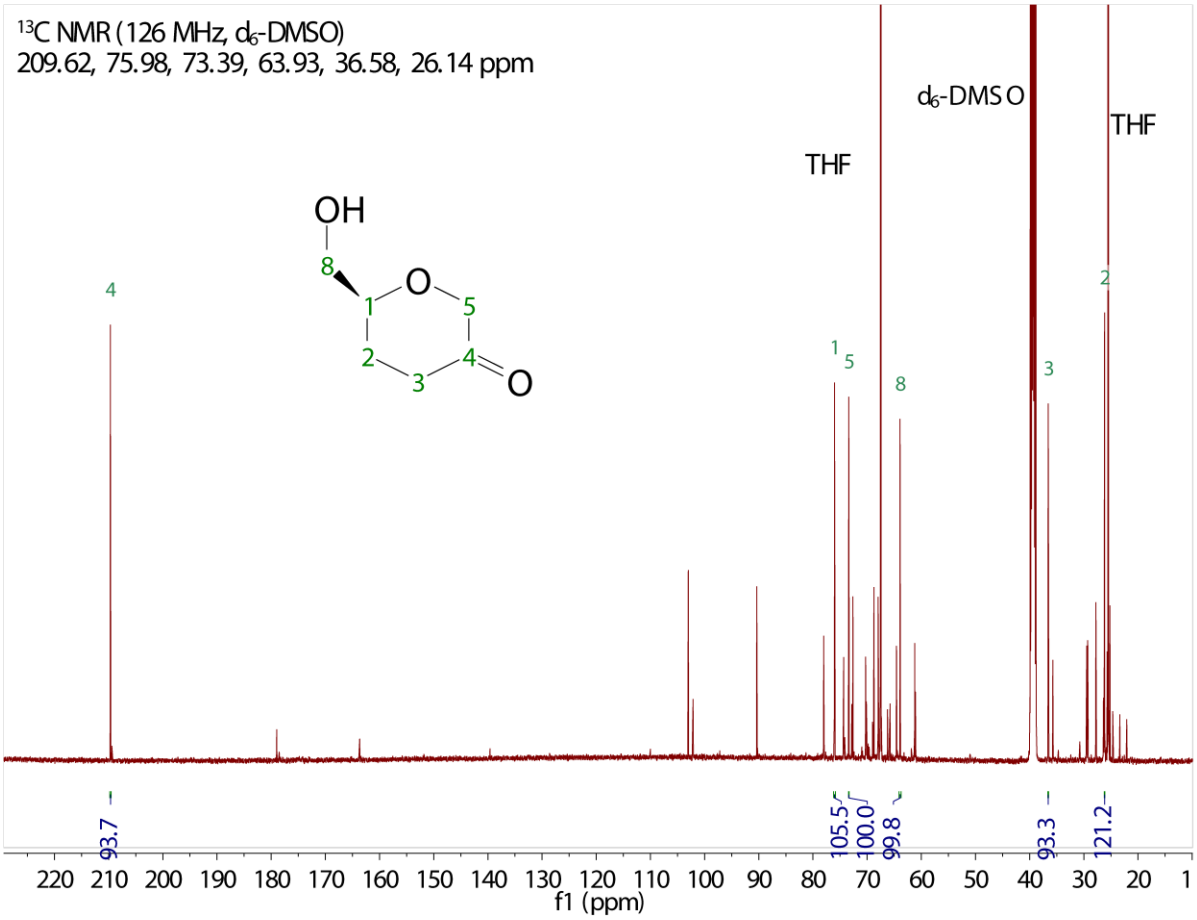

Figure S3: Quantitative ^{13}C NMR spectrum of THP2M5one-rich product, produced via acid-catalyzed Lgol isomerization (d_6-DMSO, Lgol, residual THF solvent, and other side-products are also present). Multiplicities were confirmed using polarization transfer (DEPT) experiments.

Measured chemical shifts agree with the literature.[6]

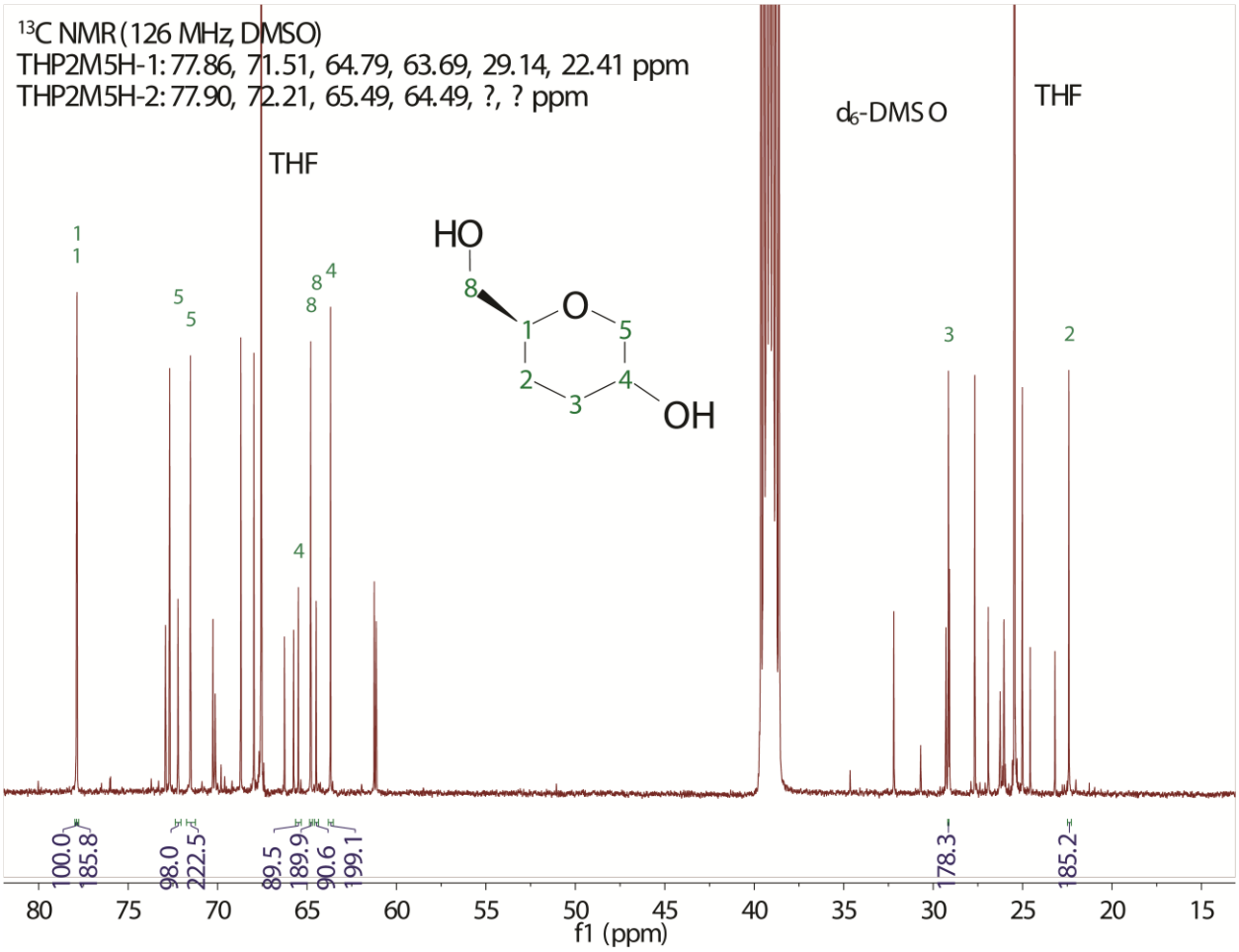

Figure S4: Quantitative ^{13}C NMR spectrum of THP2M5one hydrogenation final product (d_6-DMSO, Lgol, residual THF solvent, and other side-products are also present). The two isomers of THP2M5H were identified using this spectrum. Multiplicities were assigned using polarization transfer (DEPT) experiments. The two up-field carbons present in THP2M5H-2 could not be assigned due to the presence of impurity peaks.

The Mestrenova-predicted ^{13}C NMR spectrum of THP2M5H predicts the following chemical shifts: 77.19, 70.29, 67.06, 65.72, 30.08, 28.71 ppm. These are in good agreement with the chemical shifts in our measured spectrum.

3. CO Chemisorption

CO chemisorption was used to count the number of active sites for supported Pd catalysts, as shown in Table S1. For Pd/Al_2O_3 catalysts, the dispersion decreased as a function of increasing Pd loading, (53% dispersion at 0.4 wt%, 11% dispersion at 5 wt%). The 1% Pd/Si-Al and Pd/Al_2O_3 catalysts have similar dispersions (37% vs 42%), indicating that they have approximately similar particle sizes (3.0 nm vs 2.6 nm).

Table S1. CO Chemisorption

Catalyst	Site Density [μmol/g]*	Dispersion (%)	Approx. Particle Size (nm)**
1% Pd/C	9.7	10.4	11
5% Pd/C	104.5	22.2	5.0
0.4% Pd/Al_2O_3	21.0	53.2	2.1
1% Pd/Al_2O_3	39.1	41.6	2.6
5% Pd/Al_2O_3	51.6	11.0	10
1% Pd/Si-Al	34.5	36.7	3.0

**Assuming a stoichiometry of 1.5 Pd/CO*
*** Approximated as 1.1/D, using the CO chemisorption data and assuming spherical particles*

4. Synthesis of THP2M5one and THP2M5H

LGO Hydrogenation to Lgol

Lgol in THF was synthesized from LGO as a feedstock for Lgol hydrogenolysis. In a typical experiment, 60 mL of 50-150 mM LGO in THF feedstock was treated at 60°C for 4h over 1 g 5% Pd/C, under an atmosphere of 500 psi H_2. Quantitative conversion of LGO to Lgol was achieved, with an Lgol stereoisomer ratio of exo/endo = 1.6. The two stereoisomers of Lgol were identified by quantitative ^{13}C NMR (Figure S1).

Lgol Isomerization to THP2M5one

The acid-catalyzed isomerization of 65 mM Lgol in THF solvent (60 mL) was carried out in a batch reactor at 100°C for 3h over 400 mg Amberlyst 70 acid catalyst under inert atmosphere. 54% Lgol conversion and 61% THP2M5one selectivity were observed, with no other identifiable products. THP2M5one was identified by ^{13}C NMR (Figure S3). The resulting product solution was used as a feedstock for the experiment shown in Figure 5. This product solution was injected into the GC and HPLC. It was discovered that THP2M5one overlaps with cis-THFDM in the GC. In order to quantify cis-THFDM and THP2M5one in other experiments, the THP2M5one product was assumed to have a GC sensitivity equal to that of Lgol, allowing for the calculation of an approximate HPLC-UV sensitivity at 206 nm by comparing the GC and HPLC peak areas. THP2M5one was then quantified in other experiments using this HPLC sensitivity.

THP2M5one hydrogenation to THP2M5H

A solution containing Lgol and THP2M5one (15 mL) was generated using the acid-catalyzed isomerization of Lgol described above. This mixture was then hydrogenated at 100°C for 3h over a Pd/Al_2O_3 catalyst under 500 psi H_2 atmosphere. The Lgol was unreactive, while the THP2M5one was quantitatively hydrogenated to the two isomers of THP2M5H.

The product solution was analyzed by GC to determine the retention times for the two isomers of THP2M5H, and quantitative ^{13}C NMR was used to identify these two isomers (Figure S4). It was

discovered that the first isomer, THP2M5H-1, is overlapped with trans-THFDM in the GC, thereby requiring the deconvolution methods discussed below.

5. Product Peak Deconvolution

Quantification of cis-THFDM, trans-THFDM, THP2M5one, and the two isomers of THP2M5H is made challenging by the fact that these compounds are chemically very similar. As shown in Figure S5, trans-THFDM is overlapped with one isomer of THP2M5H in the GC, while cis-THFDM is overlapped with THP2M5one.

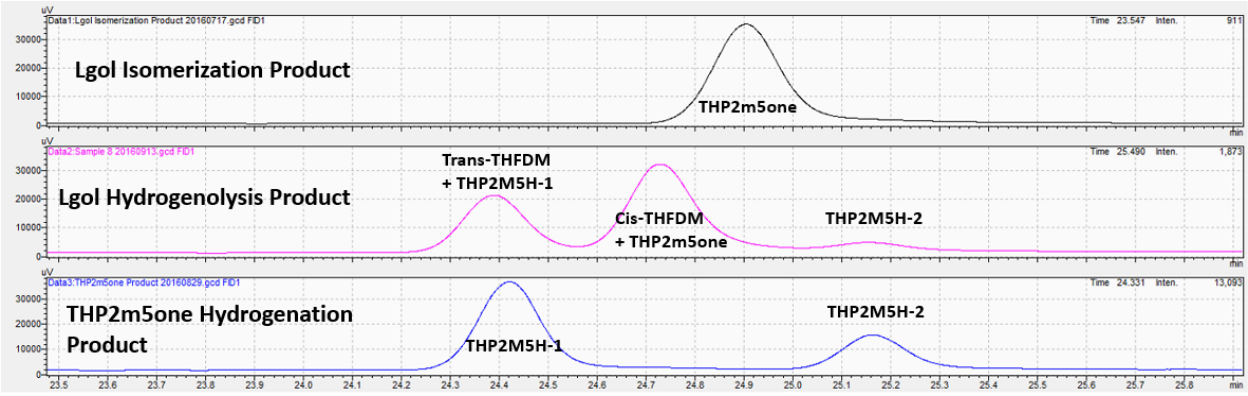

Figure S5: GC-FID chromatograms of Lgol isomerization product, Lgol hydrogenolysis product, and THP2M5one hydrogenation product.

A combination of GC, HPLC, and NMR was used to quantify these species. For experiments with concentrations over time, NMR of the final product solution was used to correct the data at earlier reaction times. The overall methodology is described in the Experimental section. An example of these calculations is shown below, for Lgol hydrogenolysis to THFDM (Figure 3).

i) Using the HPLC-UV detector at 206 nm, the THP2M5one concentration in the final product solution was calculated as 1.1 mM.

ii) The concentration of cis-THFDM in the final product was calculated by examining the GC peak corresponding to (cis-THFDM + THP2M5one) and subtracting the concentration of THP2M5one found in (i). This resulted in a cis-THFDM concentration of 20.6 mM.

iii) Quantitative ^{13}C NMR of the final product solution (Figure S2) was used to acquire the THFDM cis/trans ratio. It was found to be cis/trans = 2.45. The concentrations of trans-THFDM, THP2M5H-1, and THP2M5H-2 were found by using the known concentration of cis-THFDM (by GC) and the relative peak areas by NMR (Table S2). Note that the peak area of cis-THFDM and trans-THFDM must be divided by two because each peak corresponds to two C nucleii. The NMR peaks used for quantification were selected as peaks which were isolated in the NMR and therefore easily integrated. The concentration of THP2M5H-2, and the combined concentration of trans-THFDM and THP2M5H-1, can be measured by GC. The concentrations of these products measured by NMR can be compared to those measured by GC, and show reasonable agreement, as shown in Table S2.

^{13}C NMR spectra were run with a relaxation delay of D_1 = 15 sec. All NMR peaks used for integration (Table S2) displayed reasonable agreement in the integrated peak area. A longer

relaxation delay, D_1 = 30 sec, was used in one case and the relative peak areas did not change, verifying that the NMR quantitation is accurate.
iv) For dip-tube experiments, the concentrations of all products at earlier reaction times were corrected by assuming that the THFDM cis/trans ratio is not a function of conversion. This assumption was validated by running the Lgol hydrogenolysis reaction to intermediate conversion (53%) and verifying by NMR that the cis/trans ratio remained 2.45. Using this assumption, the true concentrations of trans-THFDM, THP2M5H-1, and THP2M5H-2 could be calculated at all reaction times. Then, the total concentrations of THFDM and THP2M5H could be calculated.

Table S2. Product Concentrations in Final Product Solution from Figure 3

Species	**NMR Peaks used (ppm)**	**Average Relative NMR Peak Area**	**NMR Concentration (mM)**	**GC Concentration (mM)**
Cis-THFDM	80.0, 64.3, 27.4	100.8	-	20.6
Trans-THFDM	79.6, 64.2, 27.9	41.2	8.4	-
THP2M5H-1	72.2, 65.5	12.9	5.3	-
THP2M5H-2	71.5, 64.8, 63.7, 22.4	5.2	2.1	2.7
Trans-THFDM + THP2M5H-1	-		13.7	12.9

6. Solvent Degradation

Degradation of the THF solvent and BHT stabilizer under reaction conditions was studied. Under the reaction conditions specified in Table 2, with 100 mg 1% Pd/Si-Al catalyst and 10 mL of THF solvent, THF was degraded in 0.7% yield to 1-butanol via ring-opening hydrogenation. A second product, 4-butoxy-1-butanol, (a product of THF hydrogenolysis and coupling; identified by GCMS) was detected at approximately 0.1% yield. Additionally, the BHT stabilizer was completely degraded into unknown products.

When the Lgol reactant was present, degradation of THF and BHT was negligible. For the experiment shown in Table 2 over 100 mg 1% Pd/Si-Al, the yield of 1-butanol from THF degradation was 0.06%, and no 4-butoxy-1-butanol was observed. BHT was also stable under these conditions. One explanation for this discrepancy is that when the reactant/products are present, these species are preferentially adsorbed on the catalyst active sites, preventing adsorption and reaction of THF and BHT. We note that degradation of THF and BHT may become important at higher reaction temperatures.

7. Catalyst Recycling Tests

The Pd/Al_2O_3 and Pd/Si-Al catalysts used for LGO, Cyrene, and Lgol conversion were each recycled (without reactivation) to study catalyst stability. For LGO hydrogenation, the catalyst used in the experiment shown in Figure 1 was recycled in situ by removing half (30 mL) of the product solution contained in the reactor, then pumping in 30 mL of a doubly concentrated LGO/THF feedstock using an HPLC pump. The reaction was then carried out a second time. This strategy avoided exposure of the catalyst to air. Figure S6 shows the LGO concentration over time for the fresh catalyst compared to the recycled catalyst. Under these conditions, the 0.4 % Pd/Al_2O_3 catalyst undergoes deactivation relative to the fresh catalyst. We note that with this recycling method, the product is present at half of its initial concentration (in this case, Cyrene at 27.5 mM) at the start of the reaction over the recycled catalyst. It is possible that product adsorption on the catalyst surface could affect the reaction rate.

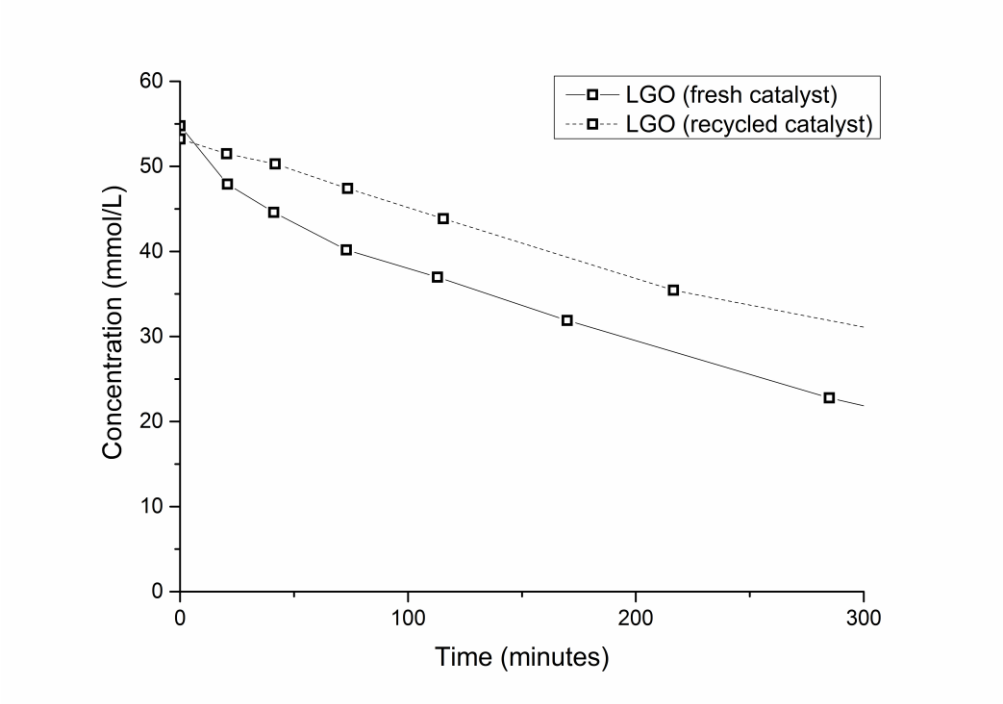

Figure S6: Catalyst recycling test for the hydrogenation of LGO over 1.75 mg 0.4 wt% Pd/Al_2O_3 (17.5 mg diluted 10x in SiO_2) in a batch reactor with dip-tube sampling. Conditions: 40°C, 500 psi H_2, 60 mL 55 mM LGO feed in THF. Lines between points are visual aids.

For Cyrene hydrogenation, the catalyst used in the experiment shown in Figure 2 was recycled in situ as described above. Figure S7 shows the Cyrene concentration over time for the fresh catalyst compared to the recycled catalyst. Under these conditions, the 0.4 % Pd/Al_2O_3 catalyst undergoes more significant deactivation relative to the fresh catalyst (compared to the case of LGO hydrogenation).

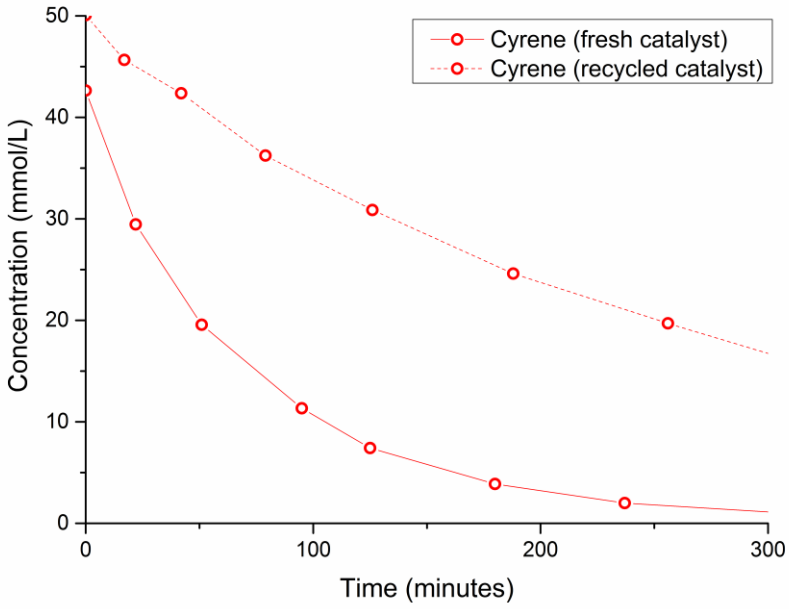

Figure S7: Catalyst recycling test for the hydrogenation of Cyrene over 150 mg 0.4 wt% Pd/Al_2O_3 in a batch reactor with dip-tube sampling. Conditions: 100°C, 500 psi H_2, 60 mL 55 mM Cyrene in THF feed. Lines between points are visual aids.

For Lgol hydrogenolysis, an experiment identical to the experiment shown in Figure 3 was conducted. The catalyst was recycled ex situ by opening the reactor, decanting the product solution, adding 60 mL of fresh Cyrene/THF feedstock, and running the reaction a second time. In situ recycling was deemed unnecessary due to the higher reaction temperature at which Pd is expected to be easily re-reduced. Figure S8 shows the Lgol concentration over time for the fresh catalyst compared to the recycled catalyst. Under these conditions, the 1 % Pd/Si-Al catalyst undergoes deactivation relative to the fresh catalyst (similar to the case of LGO hydrogenation).

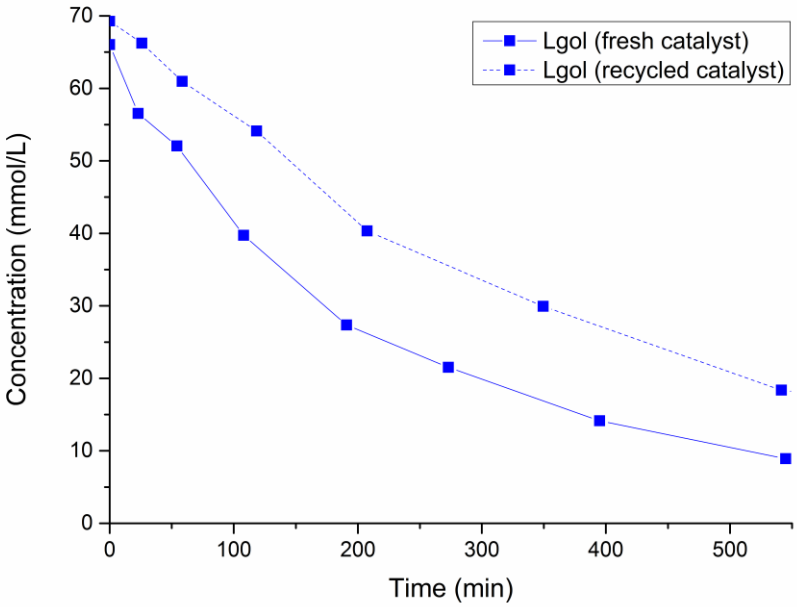

Figure S8: Catalyst recycling test for the hydrogenolysis of Lgol (exo/endo = 1.6) over 450 mg 1 wt% Pd/Si-Al in a batch reactor with dip-tube sampling. Conditions: 150°C, 500 psi H_2, 60 mL 60 mM Lgol in THF feed. Lines between points are visual aids.

References

1. M. J. Frisch, G. W. Trucks, H. B. Schlegel, G. E. Scuseria, M. A. Robb, J. R. Cheeseman, G. Scalmani, V. Barone, B. Mennucci, G. A. Petersson, H. Nakatsuji, M. Caricato, X. Li, H. P. Hratchian, A. F. Izmaylov, J. Bloino, G. Zheng, J. L. Sonnenberg, M. Hada, M. Ehara, K. Toyota, R. Fukuda, J. Hasegawa, M. Ishida, T. Nakajima, Y. Honda, O. Kitao, H. Nakai, T. Vreven, J. A. Montgomery Jr., J. E. Peralta, F. Ogliaro, M. J. Bearpark, J. Heyd, E. N. Brothers, K. N. Kudin, V. N. Staroverov, R. Kobayashi, J. Normand, K. Raghavachari, A. P. Rendell, J. C. Burant, S. S. Iyengar, J. Tomasi, M. Cossi, N. Rega, N. J. Millam, M. Klene, J. E. Knox, J. B. Cross, V. Bakken, C. Adamo, J. Jaramillo, R. Gomperts, R. E. Stratmann, O. Yazyev, A. J. Austin, R. Cammi, C. Pomelli, J. W. Ochterski, R. L. Martin, K. Morokuma, V. G. Zakrzewski, G. A. Voth, P. Salvador, J. J. Dannenberg, S. Dapprich, A. D. Daniels, Ö. Farkas, J. B. Foresman, J. V. Ortiz, J. Cioslowski and D. J. Fox, *Gaussian 09, Revision C.01*, Gaussian, Inc.: Wallingford, CT, 2009.
2. NIST Chemistry WebBook, http://webbook.nist.gov/, (accessed 10/1/16, 2016).
3. D. W. Rogers, Y. Zhao, M. Traetteberg, M. Hulce and J. Liebman, *The Journal of Chemical Thermodynamics*, 1998, **30**, 1393-1400.
4. M. S. Miftakhov, I. N. Gaisina, F. A. Valeev and O. V. Shitikova, *Russian Chemical Bulletin*, 1995, **44**, 2350-2352.

5. T. J. Connolly, J. L. Considine, Z. Ding, B. Forsatz, M. N. Jennings, M. F. MacEwan, K. M. McCoy, D. W. Place, A. Sharma and K. Sutherland, *Organic Process Research & Development*, 2010, **14**, 459-465.
6. A. Tagirov, I. Biktagirov, Y. Galimova, L. Faizullina, S. Salikhov and F. Valeev, *Russian Journal of Organic Chemistry*, 2015, **51**, 569-575.